Intra- and Intermolecular Cation–π Interactions between Onium Salts and Alkynes/Acetylene: Experimental and Theoretical Insights

Catherine Fressigné, Alexandre Jean, Morgane Sanselme, Jérôme Blanchet, Jacques Rouden, Jacques Maddaluno, Michaël de Paolis

Intra- and Intermolecular Cation–π Interactions between Onium Salts and Alkynes / Acetylene: Experimental and Theoretical Insights

Catherine Fressigné,*[,a] Alexandre Jean,[a,b] Morgane Sanselme,[c] Jérôme Blanchet,[b] Jacques Rouden,[b] Jacques Maddaluno[a] and Michaël De Paolis*[,a]

[a] Univ Rouen Normandie, INSA Rouen Normandie, CNRS, Normandie Univ, COBRA UMR 6014, INC3M FR 3038, F-76000 Rouen, France.
[b] LCMT, ENSICAEN et Université de Caen Basse-Normandie, CNRS ; 6 bd du Maréchal Juin, 14050 - Caen, France
[c] Univ Rouen Normandie, Normandie Univ, SMS , UR 3233, F-76000 Rouen, France

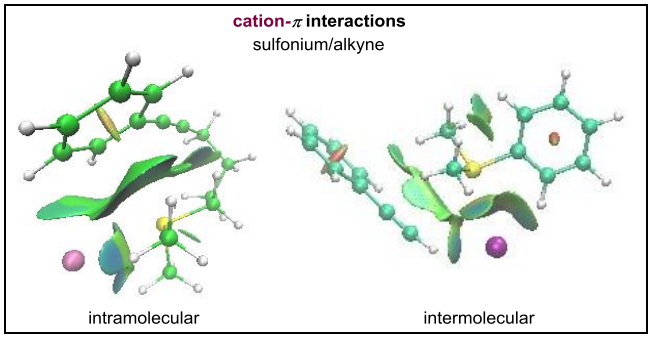

ABSTRACT Cation–π interactions between various onium salts, alkynes and acetylene were studied, taking into account the substituents of the triple bond, the nature of the anions and the polarity of the solvent, through a combination of MP2 calculations and experiments. In an intramolecular setting, these data (including single-crystal X–ray crystallography) concurred with the stability of folded conformers of alkynyl onium salts, even substituted with electron-withdrawing groups. To examine the contribution of these interactions on the alkyne electronic population, a thorough in silico study was carried out using Natural Bonding Orbital (NBO) analysis of the conformers. Intramolecular interactions from sulfonium salt tethered to phenylalkyne were highlighted, as illustrated above by the computed folded conformation (MP2) along with Non Covalent Interactions (NCI) analysis. Further, investigations of intermolecular interactions, involving acetylene or phenylacetylene with various onium ions, revealed the high energy interactions of their complexes with phenyldimethylsulfonium chloride, as illustrated above with the complex PhC≡CH/$PhMe_2SCl$ (MP2 calculations and NCI analysis).

INTRODUCTION

CH–π interactions are weak hydrogen bonds affecting the conformation of (bio)molecules and catalysts.[1] When emanating from quaternary (or tertiary) onium salts, these are described as cation–π interactions, playing an important role in several chemical and biological mechanisms.[2] In interaction with arenes or carbonyl groups, onium salts contribute to a number of catalytic (asymmetric) transformations, as well as to supramolecular assemblage and molecular recognition.[3]

Combined with alkynes, quaternary ammonium fluoride or hydroxide salts (*n*-Bu_4NX, X = F, OH) were described to promote the heterocyclization of acetylenic derivatives in basic conditions, raising the underlying question of the activation of a triple bond by noncovalent interactions.[4]

While it is expected that oniums interact with alkynes in view of their electrostatic potential surfaces, little is actually known of their strength, the implications and consequences on the triple bond reactivity. Even less is known when the nature of the onium, the anion and the polarity of the solvent are examined or when substituted alkynes are considered.

In spite of the complexity of taking in account these parameters, there are strong incentives for investigating, both intra- and intermolecular, interactions of variously substituted alkynes with onium salts (Figure 1). First, alkyne is a versatile group for bioorthogonal ligation and synthetic transformations, either as an electrophile or nucleophile.[5] A case in point, acetylene is an important C2 building block, raising stakes for storage and purification. Second, the function is a recurring template in organic materials and in

supramolecular science, applied to the design of molecular devices for example. As additional incentive, onium salts are readily available and recovered, modular and potentially chiral.

Herein is disclosed a thorough study documenting the strength and consequences of these interactions with various alkynes, oniums and anions in polar and nonpolar solvents.

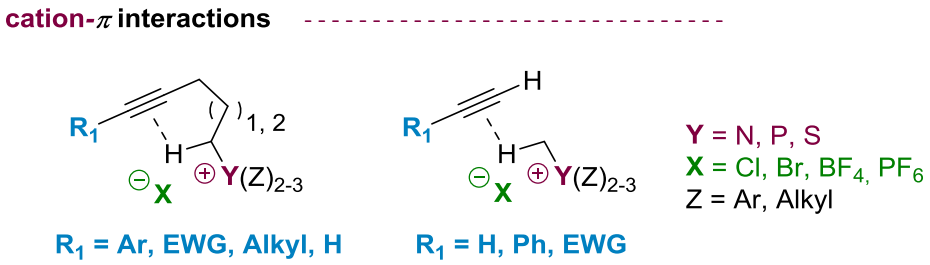

Figure 1. Consequences of the nature of oniums, anions and the solvent polarity on intra- and intermolecular interactions with alkynes.

RESULTS AND DISCUSSIONS

A. Intramolecular interactions: Inspired by the elegant design of molecular balances to study noncovalent interactions,[6] we began assessing the geometry of alkynyl ammonium salt such as **3**, reasoning that cation–π interactions could contribute to a folded conformation characterized by X–ray crystallography (Scheme 1). Pleasingly, a crystal structure of **3** provided a snapshot of a folded conformer with a 1,5–contact (distance H^{12}/C^{9} of 2.5 Å) probably due to a contribution of cation–π interactions, both intra- and intermolecular, in the packing structure. Whether computational methods could account for such binding geometries was then investigated. To that end, onium **4** was first computed without anions (Scheme 1C), at a high DFT B3P86/6–31++G** level and checked at a post-Hartree-Fock MP2/6–31++G** level (second-order Møller–Plesset perturbation theory, gas-phase).[7] As three folded conformers were computed against the linear one (see the SI), both methods confirmed the

stability (– 2.4 kcal.mol^{-1} DFT, ΔE = – 4.1 kcal.mol^{-1} MP2, ΔG = – 4.4 kcal.mol^{-1} MP2) of the folded conformer of **4** with a two-point 1,5–contact (C–H distance of 2.4 Å).

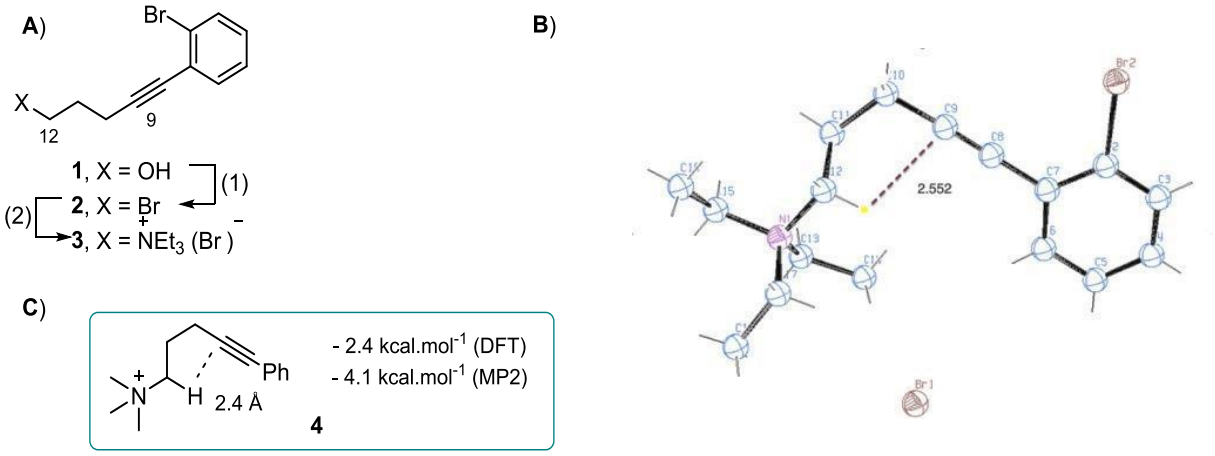

Scheme 1. **A)** Preparation of **3**; Reagents and conditions: (1) PPh_3, Br_2, CH_2Cl_2, 10 °C, 79% yield; (2) Et_3N, CH_3CN, 80 °C, 47% yield; **B)** X–ray diffraction of **3** (ORTEP, thermal ellipsoids with 50 % probability); **C)** Calculated energy stability (DFT B3P86/6–31++G** and MP2/6–31++G**) of the most stable conformer of alkyne **4** with respect to the optimized linear one.

Despite a different polarisation of the triple bond, methyl alkyne **5** and methyl alkynoate **6** tethered to ammonium cations were computed more stable as folded (– 1.9 kcal.mol^{-1}; 3.4 kcal.mol^{-1}, Figure 2), as well was **7a**, a phenylalkynyl tethered to the ammonium by a longer (n+1) carbon chain, adopting a geometry (– 3.3 kcal.mol^{-1}) with four-point contacts (1,6–: 2.4 Å; 1,9–: 2.9 Å).

To assess the implications of the solvent polarity and the nature of the anions, MP2 calculations were performed 1) in a polar solvent such as *N*,*N*-dimethylformamide (DMF continuum CPCM) then in the gas phase, and 2) with chloride, as a small anion with a centred negative charge, then with tetrafluoroborate, as a weak Lewis base (Figure 3).

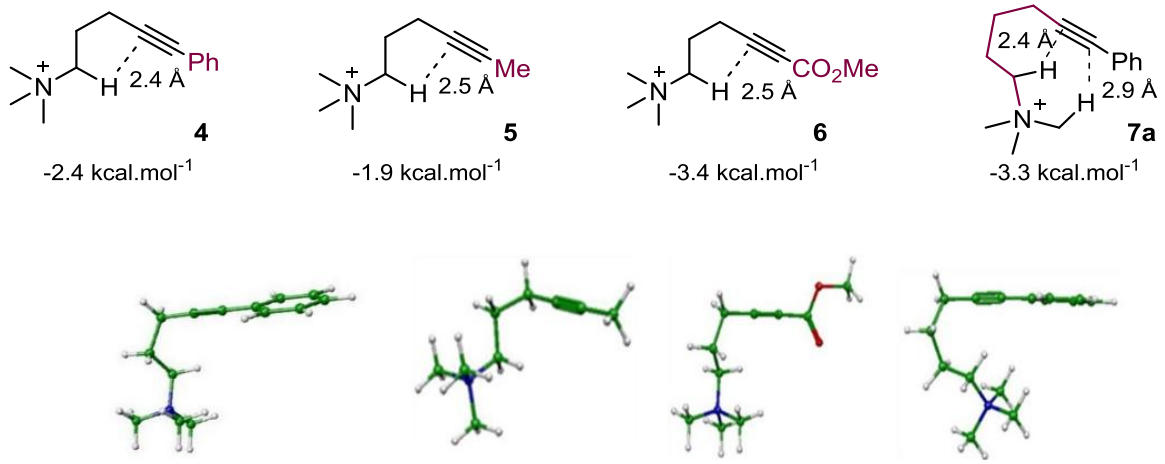

Figure 2. Energy stability (ΔE = E more stable isomer – E less stable isomer, in kcal.mol^{-1}) between the most stable folded conformations of **4a**-**7a** and the unfolded ones, calculated at DFT B3P86/6–31++G** level (gas-phase)

To limit steric bias, ammonium **7a** was selected due to the longer carbon chain connecting the two functions. To perform the conformational search, three folded conformers were computed against the linear one. Furthermore, the anions were positioned either 1) near the cation, 2) between the triple bond and the cation, or 3) close to the triple bond (see the SI for details). The unfolded conformers were computed with the chloride anion in the vicinity of the cation.

To estimate the electronic population of the alkyne, Natural Bonding Orbitals (NBO, version 3.1) analysis was performed over the optimized conformers, enabling thus a comparison with the all-carbon phenylalkyne **7b** (Fig. 3B).[8] To take into account the principle of Curtin-Hammett, the alkyne electronic population of all conformers was computed, regardless of their relative stability.

Beginning with phenylalkyne tethered to trimethylammonium chloride, the folded conformer **7a.Cl** was calculated in the gas phase as the most stable (based on the free enthalpy ΔG) compared to the unfolded one **7a.Clu** (Figure 3A). Depending on the position

of the anion, two folded conformers **7a.Cl** and **7a.Cl'** were identified with natural C^5(*sp*) charges indicating almost no electronic depletion for **7a.Cl** (+0.013 DMF/+0.003 gas-phase) and none for **7a.Cl'** (+0.001 DMF/0.000 gas-phase).

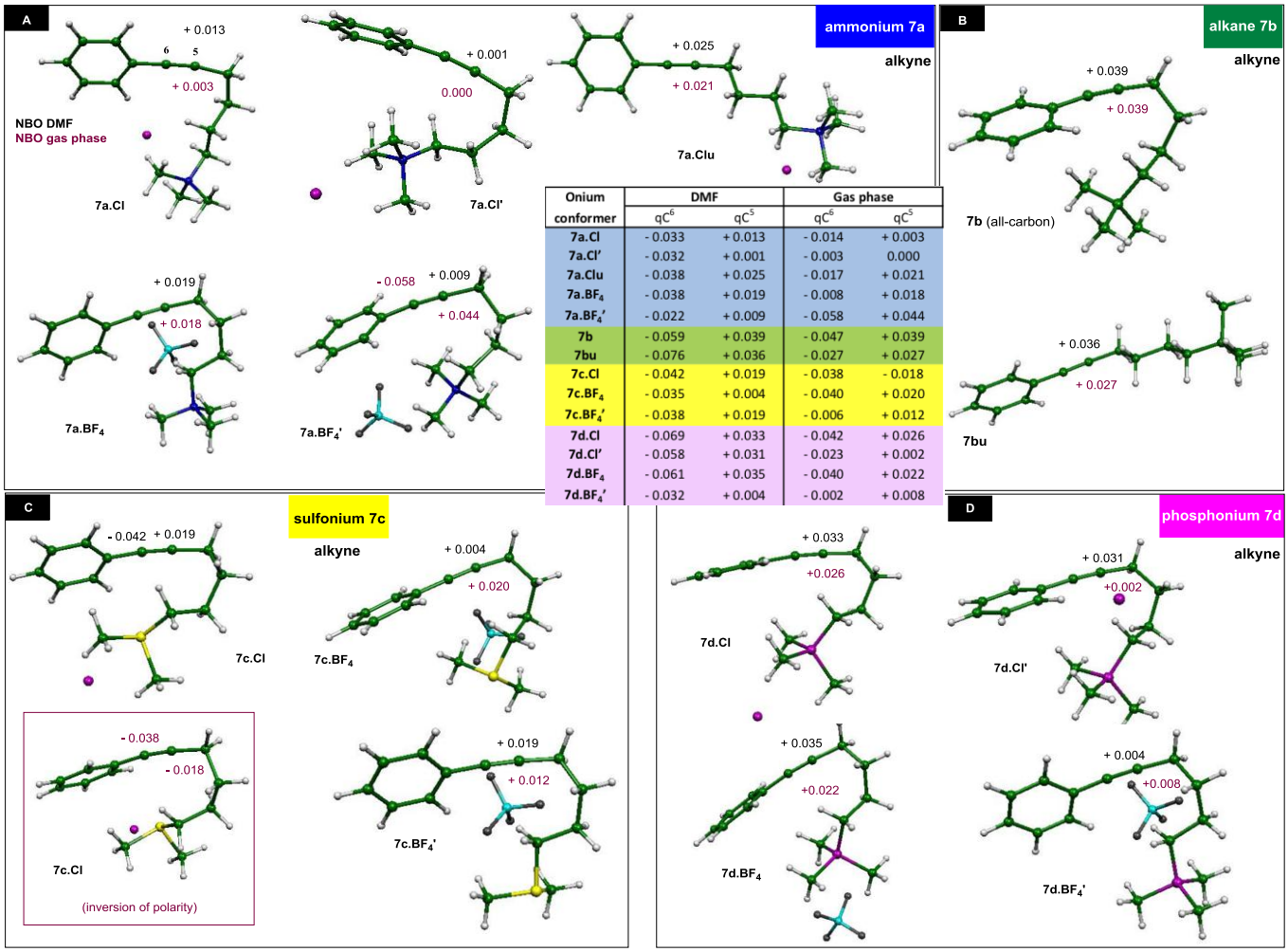

Onium conformer	DMF qC^6	DMF qC^5	Gas phase qC^6	Gas phase qC^5
7a.Cl	- 0.033	+ 0.013	- 0.014	+ 0.003
7a.Cl'	- 0.032	+ 0.001	- 0.003	0.000
7a.Clu	- 0.038	+ 0.025	- 0.017	+ 0.021
7a.BF_4	- 0.038	+ 0.019	- 0.008	+ 0.018
7a.BF_4'	- 0.022	+ 0.009	- 0.058	+ 0.044
7b	- 0.059	+ 0.039	- 0.047	+ 0.039
7bu	- 0.076	+ 0.036	- 0.027	+ 0.027
7c.Cl	- 0.042	+ 0.019	- 0.038	- 0.018
7c.BF_4	- 0.035	+ 0.004	- 0.040	+ 0.020
7c.BF_4'	- 0.038	+ 0.019	- 0.006	+ 0.012
7d.Cl	- 0.069	+ 0.033	- 0.042	+ 0.026
7d.Cl'	- 0.058	+ 0.031	- 0.023	+ 0.002
7d.BF_4	- 0.061	+ 0.035	- 0.040	+ 0.022
7d.BF_4'	- 0.032	+ 0.004	- 0.002	+ 0.008

Figure 3. Conformers of phenylalkynyl tethered to **A)** Me_3N^+ **7a**, **B)** *t*-Butyl **7b**, **C)** Me_2S^+ **7c**, and **D)** Me_3P^+ **7d** in DMF (MP2/6–31++G**, CPCM continuum). A second conformer of **7c.Cl** is shown in the gas-phase (MP2/6–31++G**). C^5 and C^6 charges by NBO analysis in DMF and gas-phase (see the enclosed Table for a comparison).

Note that the C^5(*sp*) carbon charges of the unfolded conformer **7a.Clu** (+0.025 DMF, +0.021 gas-phase) suggest that the C^5(*sp*) carbon is more electrophilic without intramolecular interactions. The folded conformer **7a.BF_4** of the trimethylammonium tetrafluoroborate

analogue (Fig. 3A) was calculated with C^5(*sp*) charges of +0.019 (DMF) and +0.018 (gas-phase). The second folded conformer **7a.BF$_4$'** was computed with almost no electronic depletion in DMF (C^5(*sp*) +0.009) while, in the gas phase, the electrophilic character (C^5(*sp*) +0.044) is increased.

By comparison, the C^5(*sp*) charge of phenylalkyne **7b** (Fig. 3B) is +0.039 (DMF and gas-phase), the unfolded conformer **7bu** has C^5(*sp*) charges of +0.036 (DMF) and +0.027 (gas-phase). Note that the folded conformer **7b** was found more stable than **7bu**, due probably to the contribution of CH-π interactions (see the SI for details).

A slight increase of the alkyne electrophilic character was only computed for **7a.BF$_4$'** (+0.044 *vs* +0.039) in the gas phase, a trend that was confirmed by Electrostatic Potential (ESP) derived charges analyses (see SI for details). Interestingly, the polarisation of the alkyne is increased with a natural C^6(*sp*) charge of – 0.058, among the highest of the series.

Phenylalkynyl dimethylsulfonium chloride **7c**.**Cl** (Fig. 3C) was next considered (in DMF, folded and unfolded conformers are isoenergetic). Note that the C^5(*sp*) carbon appeared more electrophilic (+0.019) in DMF than the ammonium counterparts **7a**.**Cl**,**Cl'**. In the gas phase, the folded conformer **7c**.**Cl** is more stable (–4.3 kcal.mol^{-1}) than the unfolded one **7c**.**Clu** and the C^5(*sp*) charge (–0.018) suggests that the carbon is electron-rich. NBO analysis of **7c**.**Clu** (see the SI) showed higher natural C^5(*sp*) charges (+0.031 DMF; +0.021 gas-phase), indicating that trialkylsulfonium-π interactions do not increase the electrophilic character of the triple bond.

On the other hand, phenylalkynyl dimethylsulfonium tetrafluoroborate salts display the usual polarisation of the triple bond in DMF (C^5(*sp*) +0.004 **7c.BF$_4$**; +0.019 **7c.BF$_4$'**) and in the gas phase (C^5(*sp*) +0.020 **7c.BF$_4$**; +0.012 **7c.BF$_4$'**). The inversion of polarity at C^5(*sp*)

was thus only noted with phenylalkynyl dimethylsulfonium chloride salts in the gas phase which was also confirmed with ESP derived charges analyses (see SI for details).

As for phenylalkynyl trimethylphosphonium chloride **7d**.**Cl** (Fig. 3D), the folded and unfolded conformers were found isoenergetic (gas-phase and DMF). With C^5(*sp*) charges of +0.033 for **7d**.**Cl** and +0.031 for **7d**.**Cl'** in DMF, the alkyne electrophilic character is close to the alkyne **7b**. In the gas phase, the electronic depletion of **7d**.**Cl** is slightly lower (C^5(*sp*) +0.026) than in the polar solvent while almost no depletion was calculated for **7d**.**Cl'** (C^5(*sp*) +0.002). The comparison with the unfolded conformer **7d**.**Clu** (C^5(*sp*) +0.028 (gas-phase); +0.033 (DMF), see the SI) suggests that **7d**.**Cl** and **7d**.**Clu** have a close electrophilic character.

Natural C^5(*sp*) charges in DMF of phenylalkynyl tethered to trimethylphosphonium tetrafluoroborate are +0.035 (**7d.BF$_4$**) and +0.004 (**7d.BF$_4$'**). In the gas phase, C^5(*sp*) charges of +0.022 (**7d.BF$_4$**) and +0.008 (**7d.BF$_4$'**) were obtained. Drawing from these numbers, the all-carbon phenylalkyne **7b** appears more electrophilic than the phosphonium salt **7d**.[9]

The fact that C^5(*sp*) charge of phenylalkynyl dimethylsulfonium chloride **7c**.**Cl** is negative in the gas phase was intriguing. To investigate this point, Non Covalent Interaction (NCI) analysis was applied to the optimized conformers (Fig. 4).[10a,b] As a topological method based on probability density and its derivatives, NCI is a convenient tool to map and study noncovalent interactions (hydrogen bonding, dipole-dipole interactions, steric repulsion and van Der Waals dispersion). Stabilizing hydrogen and ionic bonds are represented in blue, electronic or steric repulsions are visualized in red, while weak interactions are pictured in green.[10c,11]

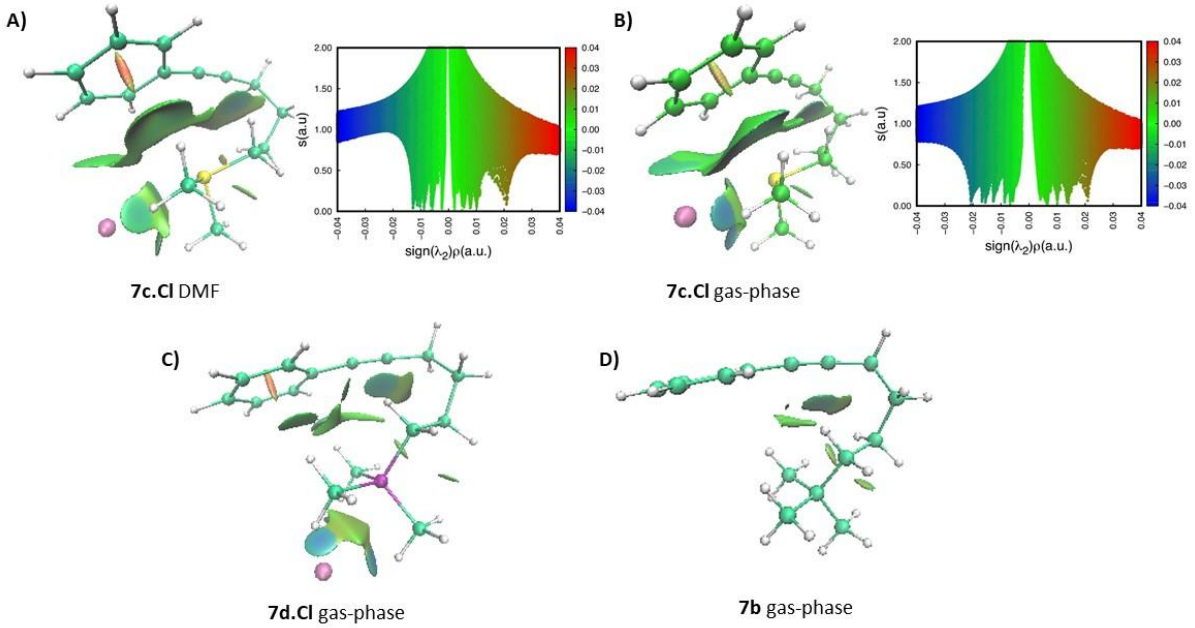

Figure 4 (A-C). Non Covalent Interaction (NCI) analysis of the optimized conformers of **A) 7c.Cl** in DMF and **B)** in gas phase with their diagrams of interactions. **C)** NCI analysis of **7d.Cl** and **D)** of **7d** in gas phase. The data were obtained by evaluating MP2/631++G** density and gradient values. The colored peaks in the 2D graph (s(r) = 0.5 isosurfaces) correspond to the regions with the same colors enclosed by the 3D isosurfaces (plots of the reduced density gradient versus the electron density multiplied by the sign of the second Hessian eigenvalue).

In the gas phase, the figure qualitatively shows the strongest interactions. Peaks picturing hydrogen and ionic bonds appear on the right side of the diagram (more electron density with negative λ2) and, as expected, these are more abundant in the gas phase. As trialkyl sulfoniums are less hindered than tetraalkyl phosphonium cations, the proximity of the sulfonium chloride salt with the phenyl (increased in gas-phase) may facilitate the interaction of the chloride anion with the phenyl connected to the alkyne. In comparison, the NCI plot of **7c**.$\mathbf{BF_4}$ shows interactions centered on the alkyne (see the SI for details) while the NCI analysis of phosphonium **7d**.**Cl**, illustrated in Fig. 4C, reveals smaller isosurfaces.

To compare the contribution of cation-π and CH-π interactions, the folded conformation of the all-carbon phenylalkyne **7b** (Fig. 4D) was analyzed, resulting in smaller NCI areas than those computed for phosphonium **7d**.**Cl** and even smaller than those calculated for sulfonium **7c.Cl**. Incidentally, no interactions were detected between the phenyl and *t*-Butyl groups of **7b**.

According to the VSEPR (Valence Shell Electron Pair Repulsion) theory, the ammonium **7a** adopts an AX_4 type geometry, a tetrahedral structure, practically without a dipole moment. While the same reasoning can be applied to phosphonium **7d**, sulfonium **7c** adopts an AX_3E geometry, a trigonal pyramidal structure with a dipole moment, which could increase the contribution of noncovalent interactions from these species.

The implications of cation-π interactions were next considered with terminal alkynes (Figure 5). A case in point, the electronic population of alkynyl trimethylammonium tetrafluoroborate **9a** was evaluated through NBO analysis (MP2/6–31++G**) in CH_2Cl_2 (continuum), a solvent of moderate polarity. The natural charges of the C(*sp*) carbons (−0.254, −0.054) from the folded conformer **9a** suggest that the electronic population is globally slightly lower than the two conformers (folded and unfolded) of 5,5-dimethylhex-1-yne (−0.300, −0.010; −0.301, −0.015), the corresponding all-carbon alkyne. The less stable unfolded conformer **9au** was computed with charges (−0.272, −0.025) indicating that **9a**, stabilized by cation-π interactions, is also globally slightly more electron-rich than **9au**. Based on the free enthalpy (ΔG) of each conformer, the Boltzmann distribution (298 K) indicates a ratio of 91:9 (**9a**:**9au**) in CH_2Cl_2.

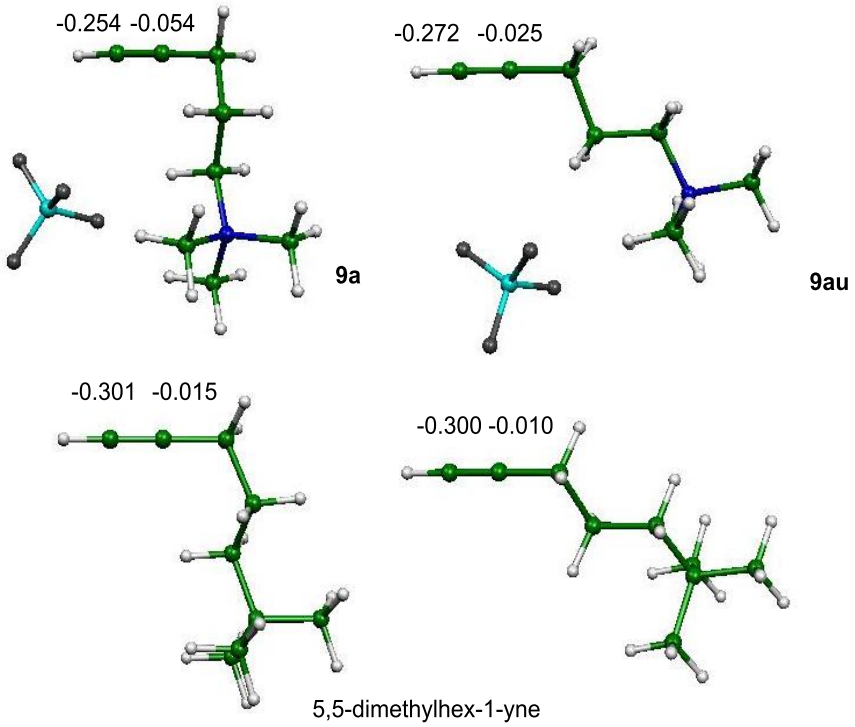

Figure 5. Optimized conformations **9a** and **9au** of terminal alkyne tethered to Me_3NBF_4 and 5,5-dimethylhex-1-yne (MP2/6–31++G**, CH_2Cl_2). Natural charges by NBO analysis

B. Intermolecular interactions: Cation-π interactions were first investigated through the complex acetylene/onium salts with a larger basis set to account for the intermolecular setting. To our knowledge, this is unprecedented as H-bonded clusters of the more acidic cation NH_4^+ and acetylene were computed, without anions, by Grabowski.[12] With this context in mind,[13-15] the study commenced with the onium salts Me_4PBF_4, Me_4PPF_6 and Me_4PX (X = Br^-, Cl^-). Interestingly, calculations (MP2/6–311++G**) showed a binding energy of the acetylene complex increasing from $PF_6^- < BF_4^- < Br^- < Cl^-$, Me_4PCl interacting with the highest energy (–10.39 kcal.mol^{-1}, Table 1, Entry 4). These values underline the cooperative role of the cation and the anion in the stabilization of the complex. Nonetheless, the contribution of the phosphonium cation was singled out with Me_4PPF_6 (–8.05 kcal.mol^{-1}) since the hexafluorophosphate anion is a weak Lewis base (Entry 2).

Table 1 Energy of interactions of complexes acetylene/Me_4P^+

Entry	Acetylene/Me_4P^+	Energy of interactions[a]
1	BF_4^-	–8.20
2	PF_6^-	–8.05
3	Br^-	–9.27
4	Cl^-	–10.39

[a] in kcal.mol^{-1}, calculated by MP2/6–311++G** in the gas phase

The complex acetylene/Me_4PBr (Figure 6A) was computed with C(*sp*) charges of –0.214 and –0.293, to compare with the complex acetylene/Me_4PBF_4 (–0.214, –0.280). In both cases, the proximity of the anion induces a polarisation of the alkyne, probably by H-bonding with HC≡CH, affecting the energy of interactions. Out of the complex, natural charges of C(*sp*) carbons (Fig. 6B) were lower (NBO charges –0.212; ESP derived charges –0.312, MP2/6–311++G** gas-phase).[16]

Quaternary ammonium salts, Me_4NBF_4 and Me_4NCl salts, were next investigated (MP2/6–311++G**) but their complexes with acetylene were less stable (–8.07 and –9.99 kcal.mol^{-1}). The contribution of the chloride anion (Me_4NCl) translated into more electron-rich C(*sp*) carbons (–0.227, –0.267) than the C(*sp*) carbons (–0.213, –0.259) of the complex with Me_4NBF_4.[17]

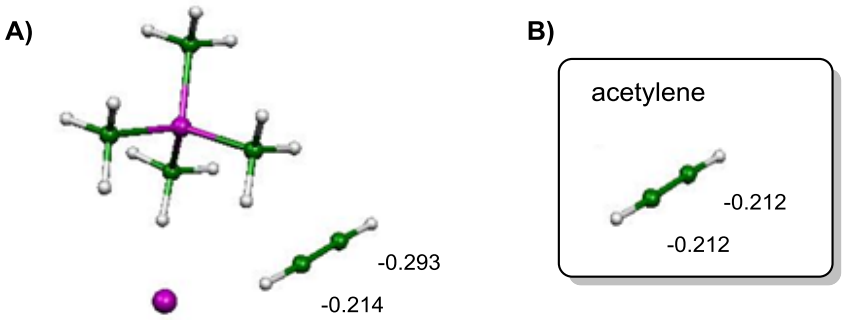

Figure 6. A) Acetylene/Me_4PBr complex, **B)** Acetylene (MP2/6–311++G**, gas-phase). Electronic populations by NBO analysis.

The complex acetylene/Me_3S^+ was investigated in pair with BF_4^-, Br^- and Cl^- anions (Table 2, MP2/6–311++G**). While the stability of the complex with Me_3SCl was highlighted (–11.05 kcal.mol^{-1}, Entry 3, and Fig. 7A), the contribution of the chloride anion, probably through H-bonding, was also underlined by the polarisation of the triple bond (–0.215, –0.306).

Table 2 Energy of interactions of complexes acetylene/Me_3S^+

Entry	Acetylene/Me_3S^+	Energy of interactions[a]
1	BF_4^-	−9.19
2	Br^-	−10.09
3	Cl^-	−11.05
4	NO_3^-	−8.12
5	HCO_2^-	−8.97

[a] in kcal.mol^{-1}, calculated by MP2/6–311++G** in the gas phase

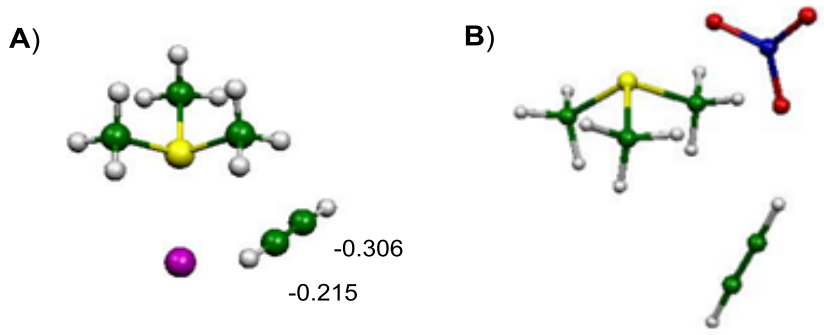

Figure 7. A) Acetylene/Me_3SCl complex, **B)** Acetylene/Me_3SNO_3 complex, (MP2/6–311++G**, gas-phase). Electronic populations by NBO analysis.

To underscore the role of the anion, Me_3S^+ was paired with a delocalized anion. With nitrate (Entry 4 and Fig. 7B), a significant drop in the binding energy of the complex (–8.12 kcal.mol^{-1}) was computed and a similar pattern was noted with the formiate anion (Entry 5, –8.97 kcal.mol^{-1}).

Interestingly, the stability of the complex could be enhanced by the sulfonium substituents.[18] Hence, higher energy of interactions was computed for the complex acetylene/$PhMe_2SCl$ (–12.31 kcal.mol^{-1} gas-phase; NBO C(*sp*) charges –0.232, –0.273; ESP derived charges –0.184, –0.400). The optimized geometry, shown in Figure 8A, illustrates the cooperative contributions of both tertiary sulfonium and chloride ions. While NBO analysis does not suggest electronic depletion of acetylene within the complex, ESP derived charges – the Merz-Singh-Kollman (MK) method – indicate that one carbon (–0.184) is more electrophilic in gas-phase. Whether the complex could remain stable in a polar solvent was evaluated and, while remaining significant, the binding energy is decreased in CH_2Cl_2 (−6.17 kcal.mol^{-1}) and DMF (–5.56 kcal.mol^{-1}). Note that in CH_2Cl_2, analysis of the C(*sp*) charges by NBO and MK, concur to suggest that there is no to little electronic depletion of the acetylene compared to the molecule outside the complex (See SI for details).

In order to characterize further the contribution, the Electron Localization Function (ELF) analysis[19] was applied to the complex acetylene/$PhMe_2SCl$ (gas-phase, Fig. 8B).

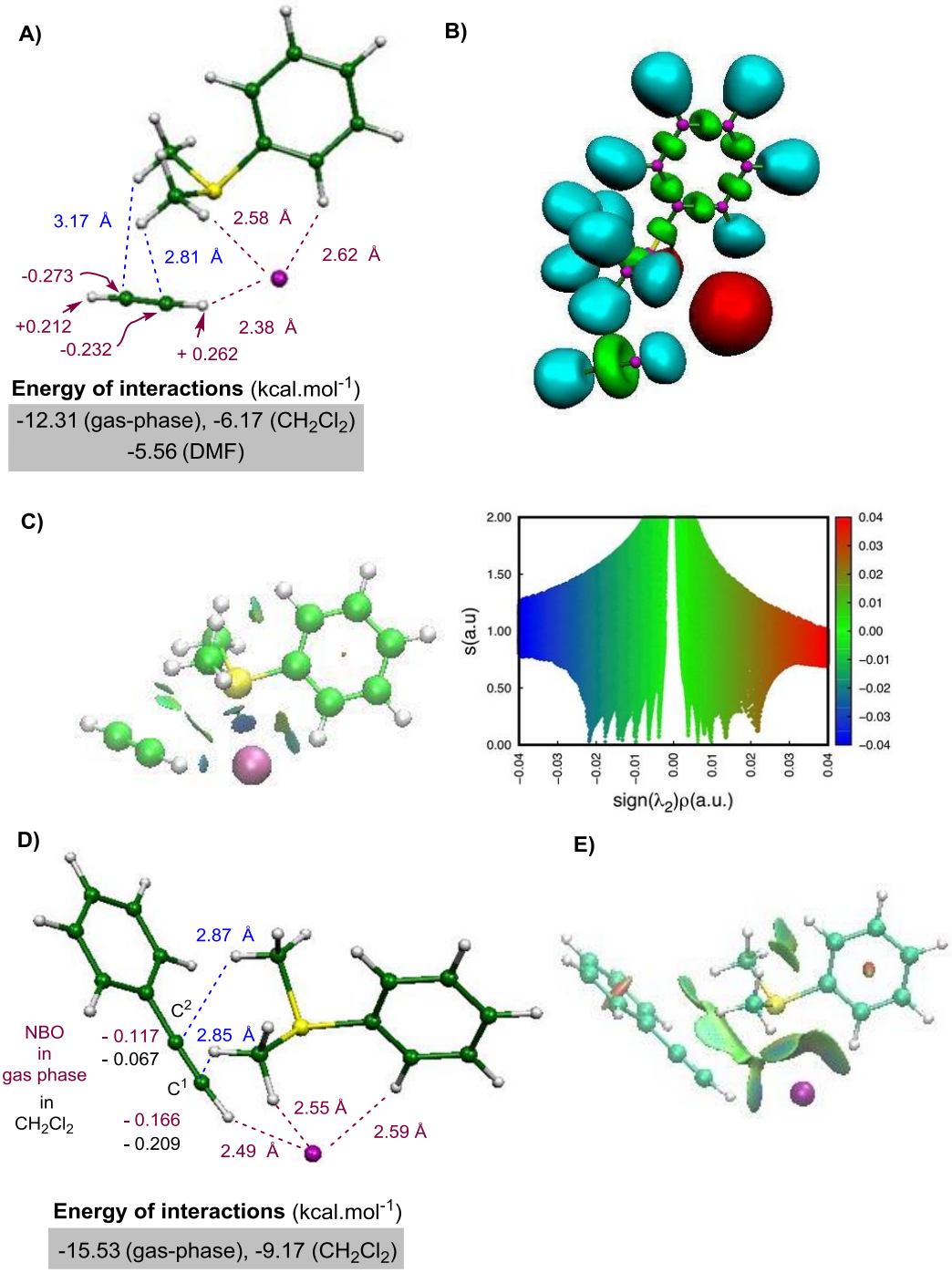

Figure 8. A) Acetylene/$PhMe_2SCl$ complex (MP2/6–311++G**, gas-phase); angle Cl-C(*sp*)-C(*sp*) 163°; distance Cl-C(*sp*) 3.42 Å; angle C(*sp*)-C(*sp*)-H 176°. Electronic populations by NBO analysis, **B)** ELF localization domains (η = 0.8) of the complex. The V(X,H) basins are

shown in turquoise, the lone pair basin in red, the core basins in magenta and the disynaptic valence basins in green. **C)** Non Covalent Interaction (NCI) plot of the complex (gas-phase), **D)** Phenylacetylene/$PhMe_2SCl$ complex (MP2/6–311++G**, gas-phase), **E)** NCI plot of the complex (gas-phase)

An interaction of the chloride ion with the C(*sp*)−H was suggested by the distance (2.38 Å) and the natural charges. Hence, the proton (+0.262) interacting with the anion is more electropositive than the second acetylene proton (+0.212), which implies the development of electrostatic interactions with the chloride ion. These values are indicative of the contribution of H to the population of the disynaptic basin V(Cl,H12), being thus very low (0.01 on a population of 1.94 electrons). Further, the noncovalent interactions from the organic cation with the acetylene π-electrons were mapped by NCI analysis (Fig. 8C). Explaining probably the higher stability of the examined complexes, hydrogen bonds with the chloride anion were pinpointed in blue, highlighting the contributions of the protons of the acetylene and the dimethylphenylsulfonium salts. Note that the resulting diagram of interactions (Fig. 8C) is similar in terms of shape and peaks to the diagram resulting from the intramolecular study (Fig. 4).

As for derivatives of acetylene, interactions of higher energy were calculated for the complexes $PhC{\equiv}CH/PhMe_2SCl$ (–15.53 kcal.mol^{-1} gas-phase, –9.17 kcal.mol^{-1} CH_2Cl_2, Fig. 8D) and $MeO_2CC{\equiv}CH/PhMe_2SCl$ (–18.13 kcal.mol^{-1} gas-phase, –8.79 kcal.mol^{-1} CH_2Cl_2, see the SI). The higher affinity of these molecules with the sulfonium salts is noteworthy, especially phenylacetylene in CH_2Cl_2. Note that the docking of methyl propiolate involves interactions with the carbonyl function (see the SI).

Within the complex in the gas phase (Fig. 8D), the triple bond of phenylacetylene is less polarized (−0.166 (C^1), −0.117 (C^2)) than the single molecule (−0.202 (C^1), −0.029 (C^2)).

In CH_2Cl_2, the alkyne polarization (−0.209 (C^1), −0.067 (C^2)) is closer to the values of the single molecule (−0.214 (C^1), −0.041 (C^2)). The trend was verified with ESP derived charges (see SI for details).

The NCI plot of PhC≡CH/$PhMe_2SCl$ (Fig. 8E) clearly illustrates the cooperative contribution of the sulfonium salt and the chloride stabilizing the complex, with a wider area than the one developed within the complex HC≡CH/$PhMe_2SCl$ shown in Fig. 8C.

To qualitatively substantiate the contribution of cation-π interactions, among other noncovalent interactions, we attempted to solubilize quaternary ammonium salts in the presence of alkyne. Hence, mixing at room temperature *n*-Bu_4NCl (15 mg) and 1-pentyne (0.2 mL), a molecule with a predicted low dielectric constant of 2.30,[20] led immediately to the solubilisation of the solids (Fig. 9A). This is indicative that noncovalent intermolecular interactions between the solute and the solvent are more favourable than the solute-solute interactions within the solids.[21]

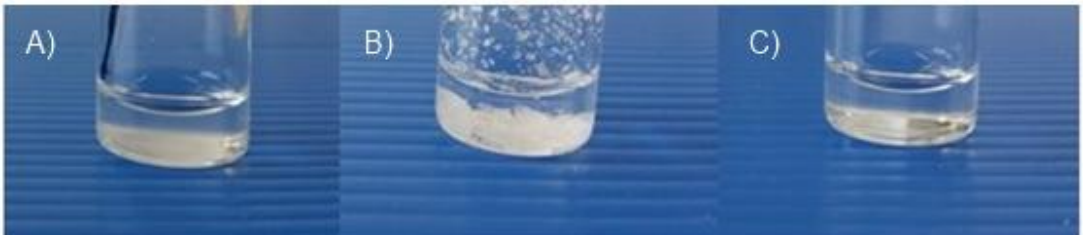

Figure 9. A) *n*-Bu_4NCl mixed with 1-pentyne, **B)** *n*-Bu_4NCl mixed with *n*-pentane, and **C)** *n*-Bu_4NBF_4 mixed with 1-pentyne, room temperature.

Conversely, mixing at room temperature *n*-Bu_4NCl (15 mg) with *n*-pentane (0.2 mL), a solvent with a low dielectric constant of 1.84, left the solids in suspension (Fig. 9B). In agreement with the "like-dissolves-like" principle, polar and charged molecules, such as *n*-Bu_4NCl, do not interact well with nonpolar solvent such as *n*-pentane.

Furthermore, *n*-Bu_4NBF_4 (15 mg) was exposed to 1-pentyne (0.2 mL) at room temperature which immediately led to a clear solution (Fig. 9C). Again, no solubilisation occurred with *n*-pentane (not shown). In the same vein, a clear solution resulted from mixing *n*-Bu_4NCl with 1-phenyl-1-butyne (not shown), a 1,2-disubstituted alkyne.

CONCLUSIONS

This study provides an unprecedented insight into cation–π interactions between various onium salts and alkynes provided by a thorough computational approach with a conformational search including the anions and taking in account the polarity of the solvents. While these interactions contributed to the folded conformation stability of the phenylalkynyl trimethylammonium and dimethylsulfonium salts **7a,c** in the gas phase, the folded and unfolded conformers of phosphonium salt **7d** were computed as isoenergetic. In a polar solvent such as DMF, folded and unfolded conformers of phenylalkynyl trimethylammonium **7a**, dimethylsulfonium **7c** and trimethylphosphonium **7d** salts were found isoenergetic at this level of theory (MP2). Among the examined salts, the binding energies (ΔG) of phenylalkynyl dimethylsulfonium chloride salts **7c.Cl** of –4.32 $kcal.mol^{-1}$ in the gas phase and +0.63 $kcal.mol^{-1}$ in DMF are noteworthy and illustrative of attractive interactions from tertiary sulfonium cations.

Whether the electrophilic or nucleophilic character of the triple bond is enhanced was investigated by examining the electronic population through NBO analysis. An increase of the alkyne polarisation of phenylalkynyl trimethylammonium tetrafluoroborate **7a**.$\mathbf{BF_4}$' was detected in the gas phase, characterized by a slight electronic depletion at the electrophilic carbon concomitant to an increase of the electronic population at the nucleophilic one. In any other scenario, the interactions induced a low polarisation of the phenylalkyne group.

As for terminal alkyne tethered to trimethylammonium tetrafluoroborate, noncovalent interactions stabilized the folded conformer **9a** in CH_2Cl_2. Compared to the all-carbon analogue, 5,5-dimethylhex-1-yne, the alkyne electronic population of both conformers, folded **9a** and unfolded **9au**, is slightly decreased, especially **9au** without cation-π interactions.

From this basis, the study was extended to intermolecular interactions of onium salts with acetylene and derivatives. In the gas phase, significant binding energies were calculated between tertiary sulfonium chloride salts, acetylene and phenylacetylene. The contribution can even be enhanced by tuning the nature of the substituent, the optimized complex acetylene/$PhMe_2SCl$ being more stable than with Me_3SCl, and the anion chloride the most binding. Interestingly, a stable complex phenylacetylene/$PhMe_2SCl$ (–9.17 kcal.mol^{-1}) was computed in CH_2Cl_2.

Within the series of analysed complexes, alkynes were, in general, not calculated more electrophilic than outside the complex, especially when taking in account the solvent. In any case, these attractive interactions could play a significant role in molecular preorganization, enabling an assemblage of electrophile and nucleophile.[22]

These findings may help in the design and tuning of molecular devices based on induced molecular geometry and incorporating the alkyne template, while enabling the understanding, the development and optimization of chemical transformations involving the building block.[23]

ASSOCIATED CONTENT

Data availability Statement

The data underlying this study are available in the published article and its Supporting Information.

CCDC1040200 contains the supplementary crystallographic data. These data can be obtained free of charge from The Cambridge Crystallographic Data Centre via www.ccdc.cam.ac.uk/data_request/cif

Supporting Information

Copies of ^{1}H and ^{13}C NMR spectra, atom coordinates and absolute energies of calculated structures, and crystal parameters of **3**.

AUTHOR INFORMATION

Corresponding Authors

Catherine Fressigné, **Alexandre Jean**, **Jacques Maddaluno** and **Michaël De Paolis** − Univ Rouen Normandie, INSA Rouen Normandie, CNRS, Normandie Univ, COBRA UMR 6014, INC3M FR 3038, F-76000 Rouen, France ; Emails : cfressig@crihan.fr, michael.depaolis@univ-rouen.fr; ORCID 0000-0001-8139-3544

Alexandre Jean, **Jérôme Blanchet** and **Jacques Rouden** − Normandie Université, ENSICAEN, CNRS, Laboratoire LCMT (UMR 6507 & FR 3038), 14000 Caen, France.

Morgane Sanselme − Univ Rouen Normandie, Normandie Univ, SMS, UR 3233, 76000 Rouen, France.

ACKNOWLEDGMENTS

The CRIANN is gratefully acknowledged for providing computation resources. We thank the CRUNCh network for a fellowship (A.J). This work has been partially supported at different stages by Normandie Université, INSA Rouen, CNRS, European Regional Development Fund (ERDF), Labex SynOrg (ANR-11-LABX-0029), Carnot Institute I2C, the graduate school for research XL-Chem (ANR-18-EURE-0020 XL CHEM), ANR (GPYRONE,

14–CE06–0016–01), ISCE–CHEM (Interreg IV, European Program), Interreg FCE LabFact (European Program and cofunded by ERDF) and by Région Normandie.

We are grateful to Prof. Anne Milet (Université de Grenoble-Alpes) for proofreading the manuscript. We thank Dr. Baptiste Picard and Dr. Mahmoud Hachem for their experimental contributions to the project at the different stages.

REFERENCES

(1) For reviews on the field, see: (a) Takahashi, O.; Kohno, Y.; Nishio, M. Relevance of Weak Hydrogen Bonds in the Conformation of Organic Compounds and Bioconjugates: Evidence from Recent Experimental Data and High-Level *ab Initio* MO Calculations. *Chem. Rev.*, **2010**, *110*, 6049–6076; (b) Nishio, M. The CH/π hydrogen bond in chemistry. Conformation, supramolecules, optical resolution and interactions involving carbohydrates. *Phys. Chem. Chem. Phys.*, **2011**, *13*, 13873–13900; (c) Späth, A.; König, B. Molecular recognition of organic ammonium ions in solution using synthetic receptors. *Beilstein J. Org. Chem.*, **2010**, *6*, 32.

(2) The term cation–π will be used to describe interactions with alkynes from C-H bonds that are vicinal to onium cation. Otherwise, these interactions are termed CH–π. For an introduction: (a) Anslyn, E. R.; Dougherty, D. A. in *Modern Physical Organic Chemistry*, (Ed. J. Murdzek), University Science Books, USA, **2006**, pp. 181–183; (b) Ma J. C.; Dougherty, D. A. The Cation−π Interaction. *Chem. Rev.*, **1997**, *97*, 1303–1324; (c) Dougherty, D. A. The Cation−π Interaction. *Acc. Chem. Res.*, **2013**, *46*, 885–893; (d) Yamada S.; Fossey, J. S. Nitrogen cation–π interactions in asymmetric organocatalytic synthesis. *Org. Biomol. Chem.*, **2011**, *9*, 7275–7281; (e) Kennedy, C. R.; Lin S.; Jacobsen, E. N. The Cation–π Interaction in Small-Molecule Catalysis. *Angew. Chem. Int. Ed.*, **2016**, *55*, 12596-12624; (f) Yamada, S. Cation−π Interactions in Organic Synthesis. *Chem. Rev.*, **2018**, *118*, 11353–11432; (g) Yamada, S., in *Noncovalent Interactions in Catalysis*, ed. K. T. Mahmudov, M. N.

Kopylovich, M. F. C. Guedes da Silva, and A. J. L. Pombeiro, The Royal Society of Chemistry, **2019**, pp. 137−152. (h) Mahadevi A. S.; Sastry, G. N. Cation−π Interaction: Its Role and Relevance in Chemistry, Biology, and Material Science. *Chem. Rev.,* **2013**, *113*, 2100−2138; (i) Yamada, S., in *The Cation-π Interaction*, Springer, **2022**.

(3) (a) Meyer, E. A.; Castellano, R. K.; Diederich, F. Interactions with aromatic rings in chemical and biological recognition. *Angew. Chem., Int. Ed.,* **2003**, *42*, 1210−1250; (b) Schneider, H. J. Binding Mechanisms in Supramolecular Complexes. *Angew. Chem., Int. Ed.,* **2009**, *48*, 3924−3977; (c) Aoki, K.; Murayama, K.; Nishiyama, H. Cation-π interaction between the trimethylammonium moiety and the aromatic ring within lndole-3-acetic acid choline ester, a model compound for molecular recognition between acetylcholine and its esterase: an X-ray study. *J. Chem. Soc., Chem. Commun.,* **1995**, 2221–2222; (d) Hughes, R. M.; Benshoff, M. L.; Waters, M. L. Influence of N-Methylation on a Cation−π Interaction Produces a Remarkably Stable β-Hairpin Peptide. *Chem. Eur. J.,* **2007**, *12*, 5753–5764; (e) Berg, L.; Mishra, B. K.; Andersson, C. D.; Ekström, F.; Linusson, A. The Nature of Activated Non-classical Hydrogen Bonds: A Case Study on Acetylcholinesterase–Ligand Complexes. *Chem. Eur. J.,* **2016**, *22*, 2672–2681; (f) Kamps, J. A. G.; Khan, A.; Choi, H.; Lesniak, R. K.; Brem, J.; Rydzik, A. M.; McDonough, M. A.; Schofield, C. J.; Claridge T. D. W.; Mecinović, J. Cation–π Interactions Contribute to Substrate Recognition in γ-Butyrobetaine Hydroxylase Catalysis. *Chem. Eur. J.,* **2016**, *22*, 1270–1276; (g) Yamada, S.; Yamamoto N.; Takamori, E. Synthesis of Molecular Seesaw Balances and the Evaluation of Pyridinium−π Interactions. *J. Org. Chem.,* **2016**, *81*, 11819-11830; (h) Cortopassi, W. A.; Kumar K.; Paton, R. S. Cation–π interactions in CREBBP bromodomain inhibition: an electrostatic model for small-molecule binding affinity and selectivity. *Org. Biomol. Chem.,* **2016**, *14*, 10926–10938; (i) Sheikh, T.; Maqbool, S.; Mandal P.; Nag, A. Introducing Intermolecular Cation-π Interactions for Water-

Stable Low Dimensional Hybrid Lead Halide Perovskites. *Angew. Chem. Int. Ed.*, **2021**, *60*, 18265–18271.

(4) (a) Yasuhara, A.; Kanamori, Y.; Kaneko, M.; Numata, A.; Kondo Y.; Sakamoto, T. Convenient synthesis of 2-substituted indoles from 2-ethynyl- anilines with tetrabutylammonium fluoride. *J. Chem. Soc., Perkin Trans. 1*, **1999**, 529−534; (b) Nagy, E.; St. Germain, E.; Cosme, P.; Maity, P.; Terentis, A. C.; Lepore, S. D. Ammonium catalyzed cyclitive additions: evidence for a cation–π interaction with alkynes. *Chem. Commun.*, **2016**, *52*, 2311–2313; (c) Fujii, A.; Choi, J.-C.; Fujita, K. Quaternary ammonium salt-catalyzed carboxylative cyclization of propargylic amines with CO_2. *Tetrahedron Lett*., **2017**, *58*, 4483−4486; (d) Jean, A.; Rouden, J.; Maddaluno, J.; De Paolis M.; Blanchet, J. Catalytic and metal-free intramolecular hydroalkoxylation of alkynes. *Tetrahedron Lett.*, **2019**, *60*, 534–537; (e) Zhao, Y.; Guo, X.; Wang, Z.; Shen, D.; Chen, T.; Wu, N.; Yan, S.; You, J. TBAF-Catalyzed Cyclization Reactions of o-(Alkynyl)phenyl Propargyl Alcohols with Malonate Esters: A Possible Cation–π Interaction as The Activation Approach. *Eur. J. Org. Chem.*, **2020**, 978–984; (f) Andoh, H.; Nakamura, K.; Nakazawa, Y.; Ikeda‐Fukazawa, T.; Okabayashi, S.; Tsuchimoto, T. Quaternary Ammonium Salts: Catalysts for Hydrosilylation of Alkynes with Hydrosilanes. *Adv Synth Catal* **2023**, adsc.202300423. https://doi.org/10.1002/adsc.202300423.

(5) (a) Gilmore, K.; Alabugin, I. V. Cyclizations of Alkynes: Revisiting Baldwin's Rules for Ring Closure. *Chem. Rev*., **2011**, *111*, 6513–6556; (b) Alonso, F.; Beletskaya, I. P.; Yus, M. Transition-Metal-Catalyzed Addition of Heteroatom−Hydrogen Bonds to Alkynes. *Chem. Rev.*, **2004**, *104*, 3079–3160; (c) Voronin, V. V.; Ledovskaya, M. S.; Bogachenkov, A. S.; Rodygin, K. S.; Ananikov, V. P. Acetylene in Organic Synthesis: Recent Progress and New Uses. *Molecules*, **2018**, *23*, 2442; (d) Chalotra, N.; Kumar, J.; Naqvi, T.; Shah, B. A. Photocatalytic functionalizations of alkynes. *Chem. Comm.*, **2021**, *57*, 11285–11300.

(6) Mati, I. K.; Cockroft, S. L. Molecular balances for quantifying non-covalent interactions. *Chem. Soc. Rev.*, **2010**, *39*, 4195–4205.

(7) See supporting information. All DFT calculations were conducted using the Jaguar 7.6 software release 211. Schrödinger, LLC, New York, 2009. All MP2 calculations were carried out with the Gaussian 09 software revision D.01.

(8) The NBO analysis was employed to estimate the carbon charges in molecular balances, see: Aliev, A. E.; Arendorf, J. R. T.; Pavlakos, I.; Moreno, R. B.; Porter, M. J.; Rzepa, H. S. Motherwell, W. B. Surfing p Clouds for Noncovalent Interactions: Arenes versus Alkenes. *Angew. Chem. Int. Ed.* **2015**, *54*, 551–556.

(9) Note that these calculations do not correlate directly with the electronegativity of the onium heteroatom as sulfur is more electronegative than phosphorus. Neither do they correlate with the pK_a of oniums (in DMSO) since sulfonium Me_3S^+ is the more acidic of the series with pK_a 24.5, their ammonium Me_4N^+ and phosphonium Me_4P^+ counterparts having pK_a of 41.9 and 26.2. Yet, the alkyne **7b** was calculated as the more electrophilic. For values of pK_a see: Fu, Y.; Wang, H.-J.; Chong, S.-S.; Guo, Q.-X.; Liu, L. An Extensive Ylide Thermodynamic Stability Scale Predicted by First-Principle Calculations. *J. Org. Chem.*, **2009**, *74*, 810–819.

(10) (a) Johnson, E. R.; Keinan, S.; Mori-Sánchez, P.; Contreras-García, J. ; Cohen, A. J.; Yang, W. Revealing Noncovalent Interactions. *J. Am. Chem. Soc.*, **2010**, *132*, 6498–6506; (b) Contreras-Garcia, J.; Johnson, E. R.; Keinan, S.; Chaudret, R.; Piquemal, J-P.; Beratan, D. N.; Yang, W. NCIPLOT: a program for plotting non-covalent interaction regions. *J. Chem. Theory Comput*., **2011**, *7*, 625-632; (c) The visualization of the isosurfaces has been performed with the VMD software: VMD for WIN32, version 1.9.1 (february 1, 2012), http://www.ks.uiuc.edu/Research/vmd/, W. Humphrey, A. Dalke, and K. Schulten, `VMD–Visual Molecular Dynamics', *J. Molec. Graphics* **1996**, 14.1, 33-38.

(11) To distinguish the nature of noncovalent interactions, the sign of the second Laplacian eigenvalue of the density $(\lambda_2)\rho$ is studied as a function of the reduced density gradient s. This value allows to characterize the "strength" of the intensity through the density. The sign of $(\lambda_2)\rho$ measures the charge accumulation in the perpendicular plane of the interaction. The function sign $(\lambda_2)\rho(r)$ enables to distinguish interaction: strongly attractive (e.g., hydrogen bonds) < 0, London dispersion ≈ 0 (irrespective of the sign) and steric clashes >0. A color code based on sign $(\lambda_2)\rho$ is often used to connect the 2D and 3D representations.

(12) Grabowski, S. J. Non-covalent interactions in $NH_4(C_2H_2)$ ammonium cation–acetylene clusters. *Comput. Theor. Chem.*, **2012**, *992*, 70–77.

(13) Cannizzaro, C. E.; Houk, K. N. Magnitudes and Chemical Consequences of R_3N^+−C−H···OC Hydrogen Bonding. *J. Am. Chem. Soc.*, **2002**, *124*, 7163–7169.

(14) Capilato, J. N.; Harry, S. A.; Siegler, M. A.; Lectka, T. Spectroscopic and Crystallographic Characterization of the R_3N^+−C−H···X Interaction. *Chem. Eur. J.*, **2022**, *28*, e202103922.

(15) (a) Shirakawa, S.; Liu, S.; Kaneko, S.; Kumatabara, Y.; Fukuda, A.; Omagari, Y.; Maruoka, K. Tetraalkylammonium Salts as Hydrogen-Bonding Catalysts. *Angew. Chem. Int. Ed.*, **2015**, *54*, 15767–15770; (b) Kaneko, S.; Kumatabara, Y.; Shimizu, S.; Maruoka, K.; Shirakawa, S. Hydrogen-bonding catalysis of sulfonium salts. *Chem. Commun.*, **2017**, *53*, 119–122.

(16) (a) Charges of – 0.228 was calculated using DFT and Natural Population Analysis (NPA), Gautam, S.; De Sarkar, A. A systematic investigation of acetylene activation and hydracyanation of the activated acetylene on Aun (n = 3–10) clusters via density functional theory. *Phys. Chem. Chem. Phys.*, **2016**, *18*, 13830–13843.

(17) Arsenium salts were examined using the same method (MP2/6–311++G**), taking in account all the electrons of the system. Interaction energies were calculated with

values of –8.03 kcal.mol^{-1} for Me_4AsBF_4 and –7.46 kcal.mol^{-1} for Me_4AsCl, suggesting a lower affinity to acetylene.

(18) Lower energies of interactions were calculated for the complexes combining **Ph$_2$**MeSCl or **Bn**Me$_2$SCl and acetylene (–11.45, –9.85 kcal.mol^{-1} MP2/6–311++G**, gas-phase). In this context, the selenium counterpart salt PhMe$_2$**Se**Cl showed significantly lower binding energy (–9.11 kcal.mol^{-1}, MP2/6–311++G**, gas-phase).

(19) The method relies on a topological approach of the chemical bond: monosynaptic and disynaptic valence basins in red (lone pair of electrons) and green, respectively, and the hydrogen atoms in blue. (a) Silvi, B.; Savin, A. Classification of chemical bonds based on topological analysis of electron localization functions. *Nature,* **1994**, *371,* 683–686; (b) Savin, A.; Silvi, B.; Colonna, F. Topological analysis of the electron localization function applied to delocalized bonds. *Can. J. Chem.*, **1996**, *74*, 1088–1096; (c) Savin, A.; Nesper, R.; Wengert, S.; Fässler, T. F. ELF: The Electron Localization Function. *Angew. Chem. Int. Ed.*, **1997**, *36,* 1808–1832; (d) The ELF analysis has been performed with the TopMod program: Noury, S.; Krokidis, X. Fuster, F.; Silvi, B. Computational tools for the electron localization function topological analysis. *Comput. Chem.*, **1999**, *23,* 597; (e) the visualization of the isosurfaces was performed with the Molekel software: MOLEKEL 4.3, Flükiger, P.; Lüthi, H. P.; Portmann, S.; Weber, J. Swiss Center for Scientific Computing, Manno (Switzerland), 2000-2002. Stefan Portmann & Hans Peter Lüthi. MOLEKEL: An Interactive Molecular Graphics Tool. CHIMIA (2000) 54 766-770.

(20) Liu, Jiangping, "Prediction of Fluid Dielectric Constants" (2011). Theses and Dissertations. 2787. https://scholarsarchive.byu.edu/etd/2787

(21) see ref. (2a), pp. 153–155

(22) This phenomenon was, for instance, characterized between azides and alkynes: Bhandary, S.; Pathigoolla, A.; Madhusudhanan M. C.; Sureshan, K. M. Azide–Alkyne

Interactions: A Crucial Attractive Force for Their Preorganization for Topochemical Cycloaddition Reaction. *Chem. Eur. J.*, **2022**, *28*, e202200820

(23) For example, the quaternary ammonium ion-tethered cycloadditions of diyne has been reported: Zhu C.; Hoye, T. R. Quaternary Ammonium Ion-Tethered (Ambient-Temperature) HDDA Reactions. *J. Am. Chem. Soc.*, **2022**, *144*, 7750–7757